Immunogenetics (2005) 57: 53–68
DOI 10.1007/s00251-004-0749-z

ORIGINAL PAPER

Alessandro Sette · John Sidney · Huynh-Hoa Bui · Marie-France del Guercio · Jeff Alexander · John Loffredo · David I. Watkins · Bianca R. Mothé

Characterization of the peptide-binding specificity of Mamu-A*11 results in the identification of SIV-derived epitopes and interspecies cross-reactivity

Received: 5 September 2004 / Revised: 10 November 2004 / Published online: 4 March 2005

Abstract The SIV-infected Indian rhesus macaque is the most established model of HIV infection, providing insight into pathogenesis and a system for testing novel vaccines. However, only a limited amount of information is available regarding the peptide-binding motifs and epitopes bound by their class I and class II MHC molecules. In this study, we utilized a library of over 1,000 different peptides and a high throughput MHC-peptide binding assay to detail the binding specificity of the rhesus macaque class I molecule Mamu-A*11. These studies defined the fine specificity of primary anchor positions, and dissected the role of secondary anchors, for peptides of 8–11 residues in length. This detailed information was utilized to develop size-specific polynomial algorithms to predict Mamu-A*11 binding capacity. Testing $SIV_{mac}239$-derived Mamu-A*11 binding peptides for recognition by peripheral blood mononuclear cells (PBMC) from Mamu-A*11-positive, SIV-infected macaques, identified five novel SIV-derived Mamu-A*11 epitopes. Finally, we detected extensive cross-reactivity at the binding level between Mamu-A*11 and the mouse H-2 class I molecule K^k. Further experiments revealed that three out of four Mamu-A*11 binding peptides which bound K^k and were immunogenic in K^k mice were also recognized in Mamu-A*11-infected macaques. This is the first detailed description of mouse-macaque interspecies cross-reactivity, potentially useful in testing novel vaccines in mice and macaques.

Keywords AIDS · SIV · MHC · Epitope · Macaque

A. Sette · J. Sidney · H.-H. Bui
La Jolla Institute for Allergy and Immunology,
San Diego, CA 92121, USA

M.-F. del Guercio · J. Alexander
Epimmune, Inc, San Diego,
CA 92121, USA

J. Loffredo · D. I. Watkins
Wisconsin National Primate Research Center,
University of Wisconsin-Madison,
Madison, WI 53715, USA

B. R. Mothé (✉)
Department of Biological Sciences,
California State University, San Marcos,
San Marcos, CA 92096, USA
e-mail: bmothe@csusm.edu
Tel.: +1-760-7503063
Fax: +1-760-7504637

Introduction

Rhesus macaques represent an important animal model for many infectious diseases, including HIV and biodefense pathogens. This model provides key insights into disease pathogenesis, and allows for the evaluation of novel vaccine concepts. Several independent observations have implicated cellular immunity, specifically cytotoxic T-lymphocyte (CTL) responses, in the control of SIV and HIV viral replication (Brander and Walker 1999; Goulder et al. 1997; Letvin et al. 1999). Recently, a renewed interest in Category A-C pathogens has revitalized efforts for developing analytical methods to rigorously analyze both cellular and humoral immune responses in non-human primates, in a number of different disease models.

The immunogenetics of rhesus macaques has only recently been explored in detail. A series of studies focused on the Mamu-A*01 class I molecule, led to the identification of its peptide-binding specificity and characterized 14 different SIV-derived CTL epitopes (Allen et al. 2001; Sidney et al. 2000). More recently, Mamu-B*17, another high-frequency allele in rhesus macaques, has been studied. The identification of the peptide-binding specificity of Mamu-B*17 resulted in the determination of 15 new SIV-derived CTL epitopes (Mothe et al. 2002b). These studies were instrumental in the synthesis of the first macaque tetramer (Kuroda et al. 1998) and enabled several different studies addressing viral evasion from CTL responses, during both the acute and chronic phases of SIV/SHIV infection (Allen et al. 2000a; Barouch et al. 2000, 2003; Chen et al. 2000; O'Connor et al. 2002; Subbramanian et al. 2003; Vogel et al. 2002). The peptide-binding specificity of other molecules,

such as Mamu-A*08, -B*03, -B*04 and -A*11 (Dzuris et al. 2000), is currently under investigation. Our ultimate goal is to allow motif searches, epitope identification studies, and production of tetrameric reagents for a number of common macaque class I and class II molecules, thus covering the majority of common MHC molecules present in the captive breeding populations utilized for vaccine and immunologic studies. Mamu-A*11 is present in the captive-bred population at a frequency of at least 5% (Rehrauer et al., manuscript in preparation; Muhl et al. 2002). Even though this allele is not as common as Mamu-A*01 and Mamu-B*17, each expressed in about 20% of the captive-bred rhesus macaque population, Mamu-A*11 can be rapidly detected using PCR-SSP (Rehrauer et al., manuscript in preparation). Mamu-A*11 therefore represents an interesting candidate for additional studies characterizing its peptide-binding motif.

Several different approaches have been utilized to predict and identify peptides bound by MHC class I molecules. Sequencing of pooled or individual naturally occurring ligands, together with the identification of the optimal T-cell epitopes, accurately reveals anchor positions and the most frequently used residues (canonical motifs) (Falk et al. 1991; Rammensee et al. 1995; Van Bleek and Nathenson 1990). However, only a subset of the good binding peptides is usually associated with canonical motifs. Indeed, peptide/MHC-binding assays with purified MHC molecules usually unveils a broader set of residues that are permissible in the anchor positions (extended motifs) (Kast et al. 1994; Kondo et al. 1995; Kubo et al. 1994; Ruppert et al. 1993; Sidney et al. 1995; Sidney et al. 1996b,c, 2000, 2001), thus allowing for a more comprehensive analysis. It has been shown that to efficiently identify MHC-binding peptides, knowledge of secondary interactions, also derived from the use of quantitative peptide/MHC-binding assays, must be taken into account (Kondo et al. 1995, 1997; Mothe et al. 2002b; Ruppert et al. 1993; Sidney et al. 1996b,c, 2000, 2001).

Characterization of naturally processed peptides has been an invaluable asset for studies attempting to define various MHC-peptide-binding motifs. This method is complementary with the use of peptide binding data, as shown in previous studies. [see, e.g. Kast et al. (1994) and Kubo et al. (1994)] Pool sequencing analysis and characterization of individual endogenous ligands have provided specific motifs for a number of MHC types. However, as shown by Kast et al. (1994) and Kubo et al. (1994) in the case of various common HLA molecules, and Sidney et al. (2000) in the case of Mamu-A*01, the motifs defined by pool sequencing studies do not represent the full range of residues that are tolerated by a particular MHC specificity in its main or secondary anchor positions. This restriction may reflect the fact that pool sequencing studies are dependent upon the pool of peptides available in the cell to MHC molecules, which may be limited or biased depending on the cellular processing capacity of the specific cell line utilized, or the rarity of specific amino acids, and only reveal the most abundant residues found at any given position.

In this study, we have performed in-depth analysis of the peptide-binding specificity of Mamu-A*11, and developed an algorithm to predict Mamu-A*11 binding. Using high-throughput binding assays and peripheral blood mononuclear cell (PBMC) samples from SIV-infected animals, we have also identified five novel SIV-derived Mamu-A*11 epitopes. Interestingly, we found that the Mamu-A*11 binding specificity overlaps with those of H-2 K^k and the HLA-B44-supertype. We have explored this potential cross-reactivity by showing that Mamu-A*11 binders also bind K^k, and that a subset of the Mamu-A*11 immunogenic peptides can elicit $CD8^+$ T-cell responses in H-2 K^k mice. This cross-reactivity between mice and macaques may be useful for performing evaluations of epitope-based approaches in mice before moving to more laborious and expensive macaque studies.

Methods and materials

Rhesus macaques, viruses, and infections

The Indian rhesus macaques (*Macaca mulatta*) used in this study were identified as Mamu-$A*11^+$ by the technique of sequence-specific DNA amplification (PCR-SSP), as previously described (Knapp et al. 1997). Of all the animals used in this study, animal 95096 was previously immunized with a liposome construct which failed to engender any immune responses after vaccination (Mothe et al. 2002a). Animals 95096 and 1937 were infected with $SIV_{mac}239$/nef open, receiving ten 50% monkey infectious doses, comprising approximately 3,000 50% tissue culture infective doses ($TCID_{50}$), intrarectally, as previously described (Allen et al. 2002a; Mothe et al. 2003; O'Connor et al. 2003). Animal 97089 was infected intravenously with 100 $TCID_{50}$ of the 3×SIV stock, which is an engineered CTL variant virus based on $SIV_{mac}239$ (Friedrich et al. 2004). Animal AJ11 was challenged three times with 300 $TCID_{50}$ $SIV_{mac}239$, intrarectally, before infection was detected (McDermott et al. 2004). The SIV-infected animals were maintained at the University of Wisconsin were cared for in accordance with an experimental protocol approved by the University of Wisconsin Research Animal Resource Committee.

Peptides

Peptides for general screening were purchased as crude material from either Pepscan Systems (Lelystad, The Netherlands) or Mimotopes (Clayton, Australia), or synthesized at Epimmune (San Diego, Calif., USA) using standard tertiary butyloxycarbonyl or fluronylmethyloxycarbonyl solid phase methods (Ruppert et al. 1993). Peptides were resuspended at 4–20 mg/ml in 100% DMSO, then diluted to required concentrations in PBS 0.05% NP40. Peptides for use as radiolabeled probes were purified to >95% homogeneity by reverse phase HPLC, and composition ascertained by amino-acid analysis, sequencing, and/or mass spectrometry analysis. Radiolabeling was done using the

chloramine T method (Sidney et al. 1998). SIV peptides utilized were derived from the $SIV_{mac}239$ sequence (accession no. M33262).

MHC purification and peptide-binding assay

A source of Mamu-A*11 molecules was provided by 721.221 cells transfected with Mamu-A*11 cDNA. The mouse B-cell lymphoma CH27 was used as the source of H-2 K^k molecules. Cells were maintained and class I MHC molecules were purified from cell lysates by affinity chromatography as previously described (Sidney et al. 1998). Mamu-A*11 molecules were purified with the anti-HLA (A, B, C) antibody W6/32 (American Type Culture Collection ATCC, Manassas, Va., USA). H-2 K^k molecules were purified using the anti-H-$2^{b,k,q,r,s}$ monoclonal antibody Y-3 (ATCC, Manassas, Va.). Protein purity, concentration, and effectiveness of depletion steps were monitored by SDS-PAGE.

Quantitative assays for the binding of peptides to detergent solubilized Mamu-A*11 and H-$2K^k$ molecules were based on the inhibition of binding of a radiolabeled standard probe peptide utilizing the same protocol described for the measurement of peptide binding to HLA class I molecules (Sidney et al. 1998). Briefly, 1–10 nM of radiolabeled peptide was co-incubated at room temperature with 1 μM to 1 nM of purified class I molecules in the presence of 1 μM human β_2-microglubulin (Scripps Laboratories, San Diego, Calif.) and a cocktail of protease inhibitors. The radiolabeled peptide utilized for Mamu-A*11 assays was the previously identified Mamu-A*11-restricted $CD8^+$ T-cell epitope SIV Env 495–502 (sequence GDYKLVEI) (Evans et al. 1999). The radiolabeled peptide for H-2 K^k assays was an artificial consensus sequence (SEAAYAKKI) derived from an analysis of the sequences of known K^k-restricted CTL epitopes or endogenously bound ligands.

After a two-day incubation, binding of the radiolabeled peptide to the corresponding class I molecule was determined by capturing MHC/peptide complexes on Optiplates (Packard Instrument, Meriden, Conn., USA) coated with either the W6/32 (for Mamu-A*11 assays) or Y-3 (for H-2 K^k assays) antibody, and measuring bound cpm using the TopCount microscintillation counter (Packard Instrument). In the case of competitive assays, the concentration of peptide yielding 50% inhibition of the binding of the radiolabeled probe peptide was calculated. Peptides were typically tested in three or more independent experiments. Since under the conditions utilized, where [label] < [MHC] and $IC_{50} \geq$ [MHC], the measured IC_{50} values are reasonable approximations of the true K_d values. In each experiment, a titration of the unlabeled version of the radiolabeled probe was tested as a positive control for inhibition.

Bioinformatic analyses

For detailed analysis of the peptide binding data and to allow comparison of data obtained in different experiments, a relative binding value was calculated for each peptide assayed by dividing the IC_{50} of the positive control for inhibition by the IC_{50} for each tested peptide. These standardized relative binding values also allow the calculation a geometric mean, or average relative binding (ARB) value, for all peptides of a particular characteristic (Gulukota et al. 1997; Kondo et al. 1995, 1997; Mothe et al. 2002b; Ruppert et al. 1993; Sidney et al. 1996b,c, 1998, 2000). The binding capacity of peptides in each size group (8, 9, 10, or 11 residues) was analyzed by determining the ARB values for peptides that contain specific amino-acid residues in specific positions. For determination of the specificity at Mamu-A*11 main anchor positions, ARB values were standardized relative to the ARB values of peptides carrying the residue associated with the best binding. For secondary anchor determinations, ARB values were standardized relative to the ARB of the whole peptide set considered. Because of the rare occurrence of certain amino acids, residues were grouped according to individual chemical similarities, as previously described (Gulukota et al. 1997; Kondo et al. 1995, 1997; Mothe et al. 2002b; Ruppert et al. 1993; Sidney et al. 1996b,c, 1998, 2000), when the incidence of a given amino acid was less than 5.

A method for the derivation of polynomial algorithms using ARB values as coefficients has been described previously (Gulukota et al. 1997; Mothe et al. 2002b; Sidney et al. 1996b,c, 2000; Southwood et al. 1998). This predictive methodology is based on the assumption of the independent binding of peptide side chains, where the stability contributed by a given residue at a given position is independent of the nature of the residues at other positions. These algorithms take into account both extended and refined motifs (Gulukota et al. 1997; Ruppert et al. 1993) and are essentially based on the premise that the overall affinity (ΔG) of peptide-MHC interactions can be approximated as a linear polynomial function of the type $\Delta G = a_{1i} \times a_{2i} \times a_{3i} \times \ldots\ldots a_{ni}$, where a_{ij} is a coefficient that represents the effect of the presence of a given amino acid (j) at a given position (i) along the sequence of a peptide of n amino acids. When residue j occurs at position i in the peptide, it is assumed to contribute a constant amount j_i to the free energy of binding of the peptide, irrespective of the sequence of the rest of the peptide. To calculate the algorithm score of a given peptide in a test set, the geometric mean of all ARB values corresponding to the sequence of the peptide is calculated. If the resulting score exceeds a chosen threshold, the peptide is predicted to bind. Appropriate thresholds can be chosen as a function of the degree of stringency of prediction desired.

The performance of the predictive algorithms can be assessed by the measures of sensitivity or efficiency. Sensitivity indicates the fraction of known binders that are in fact identified using the specific algorithm, and efficiency measures the fraction of peptides predicted to be binders that actually bind (in the present context, binders were defined as peptides with affinities of 500 nM, or better). In the present study algorithms were evaluated by measuring the efficiency of prediction when the sensitivity was set at either 0.75 or 0.90. That is, the efficiency of prediction was

evaluated with library subsets that included either 75% or 90% of the peptides in the data set that bound with an IC_{50} value of 500 nM, or better.

IFN-γ ELISPOT assay for macaque PBMC

Ninety-six-well flat-bottomed plates (U-Cytech BV, The Netherlands) were coated with 5 μg of anti-gamma interferon (IFN-γ) mAb MD-1 (U-Cytech-BV) overnight at 4°C. The plates were then washed five times with PBST, PBS (GibcoBRL, N.Y., USA) containing 0.05% Tween-20 (Sigma Chemical, St. Louis, Mo., USA), and then the plates were blocked with 2% PBSA, PBS containing 2% BSA (Sigma Chemical, St. Louis, Mo.) for 1 h at 37°C. The 2% PBSA was discarded from the plates and freshly isolated PBMC were added. Cells were resuspended in RPMI-1640 (Mediatech, USA) supplemented with penicillin, streptomycin and 5% FBS (Biocell, Calif.) (R05). The R05 also contained either 10 μg/ml concanavalin A (Con-A; Sigma Chemical), 10 μg/ml of each peptide, or no peptide. Input cell numbers were 1.0×10^5 PBL in 100 μl/well, in triplicate wells.

The plates were incubated with the cells overnight (16–20 h) at 37°C, 5% CO_2. The cells were then removed by shaking them off the plates and 200 μl/well of ice-cold deionized water was added to lyse the remaining PBMC. The plates were incubated on ice for 15 min after which they were washed ten times with PBST. Next, 1 μg/well of rabbit polyclonal biotinylated detector antibody solution (U-Cytech BV) was added and the plates were incubated for 1 h at 37°C. The plates were washed five times with PBST after which 50 μl/well of a gold-labeled anti-biotin IgG solution (U-Cytech BV) was added. The plates were once again incubated for 1 h at 37°C and washed five times with PBST. Activator mix (U-Cytech BV) was then added at 30 μl/well and the plates were developed for about 5–20 min. The activator mix consists of a silver salt solution that precipitates at the sites of gold clusters (from the gold-labeled anti-biotin solution), visualizing the sites where the IFN-γ was secreted. Once these sites or black spots could be seen in the wells under an inverted microscope, the wells were washed with distilled water to stop development. The plates were then air-dried.

Wells were imaged using an AID ELISPOT reader (Strassberg, Germany). A spot-forming cell (SFC) was defined as a large black spot with a fuzzy border (Klinman 1994). To determine significance levels, the average of the number of SFCs and standard deviation for each peptide was calculated. Background (sample with no peptide) levels were subtracted from each peptide average. A response was considered positive if the average number of SFCs exceeded a threshold of 50 and the average of sample with no peptide plus 2 standard deviations. Assay results are shown as SFC p/1×10^6 cells. Responses to ConA (positive control) were always greater than 1,000 SFCs p/1×10^6 cells.

Mouse immunizations

For peptide immunization, groups of three mice were immunized by subcutaneous injection at the base of the tail with a mixture of peptides: 25 μg of each class I binding epitope/mouse; 70 μg/mouse of the helper IE^k-restricted epitope, human lambda repressor 12–27 (sequence YLE DARRLKAIYEKKK); and 70 μg/mouse of the helper IA^k- and IE^k-restricted epitope, acetylcholine receptor 195–212 (sequence DTPYLDITYHFVMQRLPL) in PBS/10% DMSO emulsified in IFA (Difco, Detroit, Mich., USA). A mouse was immunized with a maximum of 14 peptides. In this case, two different mixtures of peptides were formulated, i.e., seven class I-restricted and two class II-restricted peptides were delivered per mouse. After 11–14 days, the mice were sacrificed and the splenocytes were purified for inclusion in the ELISPOT assays.

IFN-γ ELISPOT assay for measuring ex vivo mouse $CD8^+$ T-cell responses

Enzyme-linked immunospot (ELISPOT) assays were performed according to standard protocols (Murali-Krishna et al. 1998). Briefly, 4×10^5 splenic $CD8^+$ cells isolated by magnetic beads (Miltenyi Biotec, Auburn, Calif.) and 5×10^4 L929 fibroblasts-k haplotype cells (ATCC, Rockville, Md., USA) pulsed with 10 μg/ml of peptide were cultured in flat-bottom 96-well nitrocellulose plates (Immobilon-P membrane; Millipore, Billerica, Mass., USA) which had been precoated with anti-IFN-γ mAb (BD PharMingen; 10 μg/ml). After 20 h incubation at 37°C, plates were washed with PBS/0.05% Tween and wells were incubated with a biotinylated anti-IFN-γ mAb (BD PharMingen; 2 μg/ml) for 4 h at 37°C. After additional washing, spots were developed by sequential incubation with Vectastain ABC peroxidase (Vector Laboratories, Burlingame, Calif.) and 3-amino-9-ethyl carbazole (AEC) solution (Sigma-Aldrich) and counted by computer-assisted image analysis (ZEISS KS ELISPOT Reader, Germany). To determine the level of significance, a Student's *t*-test was performed in which $P\leq0.05$ using the mean of triplicate values of immunized mice (relevant peptide response-irrelevant peptide response) versus unimmunized mice (relevant peptide response-irrelevant peptide response).

Results

Detailed characterization of the preferred ligand size and primary anchor specificity of Mamu-A*11

We have previously performed limited single substitution analysis for each amino-acid position of a known Mamu-A*11 epitope, $Env_{495\text{-}502}$GI8 (Dzuris et al. 2000; Evans et al. 1999), using a live cell binding assay, and defined a preliminary Mamu-A*11 binding motif. From the small panel of analog peptides tested, D or E at position 2, and I and

L at the C-terminus were found to be the preferred anchor residues for Mamu-A*11 binding.

Herein we report a development of a high throughput Mamu-A*11 binding assay which utilizes purified MHC molecules. With this assay we first examined a comprehensive panel of position 2 and C-terminal single substitution analogs based on the HIV gp 120 1–9 peptide (sequence AENLWVTVY). In preliminary experiments the binding affinity of the gp 120 1–9 peptide was determined to be in the 70 nM range. This level of affinity is well-suited for single substitution analysis in that it is high enough so that binding is not easily disrupted by minor substitutions, but not too high so that the potential effect of a given substitution may be lost, or overcompensated by an abundance of strong secondary influences.

For this analysis, we defined at any given position preferred residues as those whose binding capacity, relative to the binding capacity of the optimal residue, is 0.1, or better. Residues whose binding capacity is between 0.01 and 0.1 are considered tolerated. Finally, residues whose binding capacity is less than 0.01 are defined as non-tolerated.

As shown in Fig. 1a, at position 2, D and E are preferred, but the large aliphatic residue M is also tolerated. All other amino acids at position 2 were associated with relative binding capacities < 0.01, and are thereby considered non-tolerated. At the C-terminus it was found that F, I and V are preferred, and the aliphatic residues M and L, are tolerated (Fig. 1b). All other residues at the C-terminus are non-tolerated (relative binding capacities < 0.01).

Next, to define more accurately the factors influencing Mamu-A*11 binding, we investigated the binding capacity of a library of over 1,000 different naturally occurring peptides of either viral or bacterial origin. All of the peptides examined carried E, D or M in position 2, and I, L, M, V or F at the C-terminus. Based on chemical similarity, peptides with W, Y, A and T at the C-terminus were also included. Each peptide was separately tested for binding to purified Mamu-A*11 molecules, and the data analyzed for specific trends. We found that 43 of 214 (20.1%) 8-mer, 152 of 370 (41.1%) of 9-mer, 113 of 277 (40.8%) 10-mer, and 50 of 192 (26.0%) 11-mer peptides bound Mamu-A*11 with an IC_{50} of 500 nM, or better (Table 1a). Thus, we concluded that peptides of either 9 or 10 residues in length are optimal for Mamu-A*11 binding.

We also utilized the library to further analyze the main anchor ligand specificity. The effect of a specific amino-acid residue in a given position was determined by calculating the average relative binding value (ARB) (see Materials and methods) associated with each residue at that particular position. Our results confirmed the preference, noted in the single substitution analysis, for glutamic acid (E) over aspartic acid (D) at position 2 (Table 1b). Specifically, it was found that 289 of 644 (44.9%) peptides carrying E in position 2 bound Mamu-A*11 with an IC_{50} of 500 nM, or better, compared with 56/305 (18.4%) peptides containing D at the second position. The relative (to peptides with E in position 2) binding capacity (ARB) of peptides with D in position 2 was 0.021. Peptides with M in position 2 had an ARB of 0.018, and 13/104 (12.5%) were binders.

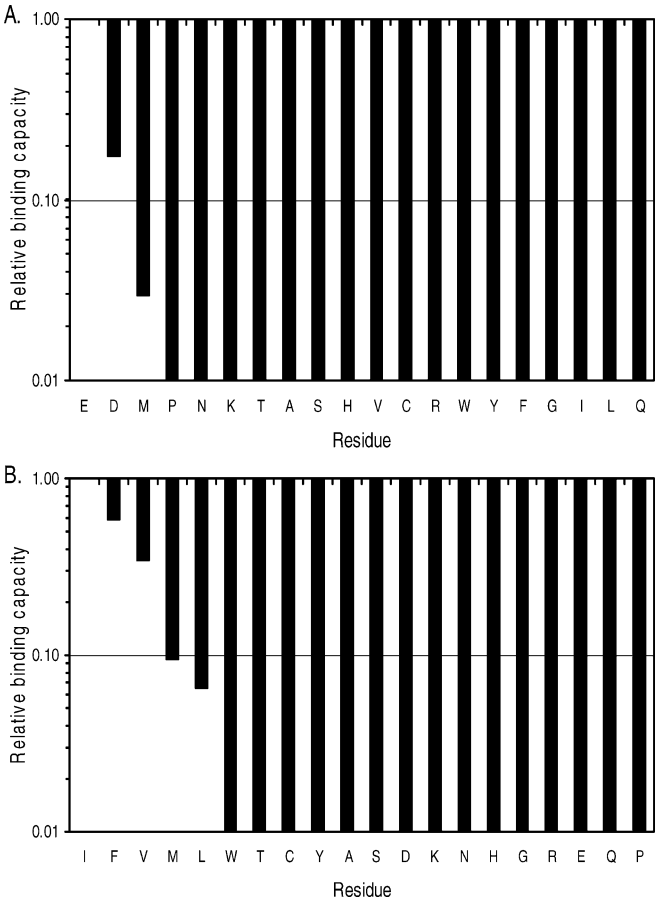

Fig. 1 Mamu-A*11 binding capacity of single amino acid substitutions at position 2 **a**. and the C-terminus **b**. of HIV gp120 1-9 (sequence AENLWVTVY). Binding is indexed relative to the residue at the same position with the highest binding capacity. Residues with relative binding capacities in the 0.1–1.0 range are considered as preferred. Residues associated with a relative binding capacity in the 0.01–0.1 range are considered as tolerated. Residues with relative binding less that 0.01 are considered as non-tolerated in the corresponding main anchor position

At the C-terminus (Table 1c), I was found to be the only preferred residue. In total, 112 of 175 (64.0%) of the peptides with I at the C-terminus bound Mamu-A*11. Other aliphatic (V, L, and M) and aromatic (F and W) residues were tolerated at the C-terminus, with ARB values in the 0.072–0.018 range, and with frequencies of binding between 23.5–37.9%. Peptides with the closely related residues A, T, and Y were found to be not tolerated (as was also the case in the single substitution analysis), with ARBs < 0.01.

In conclusion, these analyses have identified the primary specificity for Mamu-A*11, where the main anchors are in position 2 and at the C-terminus of its peptide ligands. At position 2, the acidic residue E is preferred, and D and M are tolerated. At the C-terminus, the aliphatic hydrophobic residue I is preferred, and the hydrophobic residues F, W, L, M, and V are tolerated. Mamu-A*11 has

Table 1 Primary features influencing Mamu-A*11 peptide-binding capacity

Length	*n*	Binders[a]	% binders	ARB[b]
a. Mamu A*11 binding as a function of peptide length				
8	214	43	20.1	0.15
9	370	152	41.1	1.0
10	277	113	40.8	0.70
11	192	50	26.0	0.23
Total	1053	358	34.0	
Residue	*n*	Binders	ARB	
b. Fine specificity at position 2[c]				
E	644	289		1.0
D	305	56		0.021
M	104	13		0.018
Total	1053	358		
c. Fine specificity at the C-terminus[d]				
I	175	112		1.0
V	174	66		0.072
L	245	90		0.057
M	46	14		0.043
F	95	32		0.039
W	68	16		0.018
A	66	8		–[d]
T	103	14		–
Y	81	6		–
Total	1053	358		

[a]Binders are peptides with an IC50≤500 nM
[b]ARB values are calculated as described in the Materials and Methods, and are indexed to the binding capacity of the size associated with the highest binding affinity
[c]ARB values are calculated as described in the Materials and methods, and are indexed to the binding capacity of the residue associated with the highest binding affinity
[d]Less than 0.001

a preference for 9- and 10-mer ligands, but can also bind 8- and 11-mer sequences.

The secondary anchor positions influence peptide binding to A*11

To determine if secondary influences on peptide binding to Mamu-A*11 molecules could be detected, the peptide-binding data from the library utilized above was further analyzed. Secondary anchor motifs were derived from libraries of 214, 370, 277 and 192 peptides for 8, 9, 10, and 11-mer peptides, respectively. Thus, the secondary anchor determinations were based on average of 10.7, 18.5, 13.9, or 9.6 observations for each amino acid residue in each secondary anchor position. However, due to the rarity of certain amino acids, as described in the Materials and methods section, when there were fewer than five occurrences of a certain amino acid in a specific position, the value calculated for that amino acid in that specific position was derived by grouping it with residues of similar chemical specificity. As described in the Materials and methods section, the average relative binding capacity of peptides carrying each of the 20 amino acids was calculated for each non-anchor position. These data are summarized in Table 2.

Regardless of peptide size, it was found that at most positions some positive and/or deleterious influences on peptide binding could be identified. For all sizes proline (P) and acidic residues (D and E) in position 1 had a deleterious influence. A preference for aromatic residues (F, W, and Y) in position 3 was shared between 8-, 9- and 10-mers. Other position specific commonalities in specificity were difficult to discern. However, it was noted that the majority (42/48; 87.5%) of deleterious influences were associated with polar (D, E, R, H, K, Q, N, S, T or C) or small (P and G) residues, and that the majority (44/68; 64.7%) of preferred residues were hydrophobic (F, W, Y, L, I, V, M or A). Fig. 2 provides summary maps of the data shown in Table 2.

Linear polynomial algorithms for predicting Mamu-A*11 binding

Polynomial algorithms are an effective tool for identifying peptide sequences with a good probability of binding class I molecules with high affinity. The use of ARB values as coefficients for polynomial algorithms has been described previously by our group (Gulukota et al. 1997; Mothe et al. 2002b; Sidney et al. 1996b,c, 2000; Southwood et al. 1998), and is summarized in the Materials and methods. Herein, we have applied this method to the derivation of Mamu-A*11 predictive algorithms.

A common measure of the performance of an algorithm is its efficiency (or positive predictive value), which refers to the fraction of the predicted peptides that are actually binders. The ARB values shown in Table 2 were utilized as coefficient matrices to score 8-, 9-, 10-, or 11-mer sequences, as described in the Materials and methods. Next, peptide scores were plotted against measured IC_{50} nM values and appropriate thresholds were determined to select 90 or 75% of peptides with measured IC_{50} less than 500 nM. Algorithm scores that allowed prediction of 90 or 75% of the binders in the data set analyzed are shown in Table 3 for 8-, 9-, 10- and 11-mers, respectively.

In the present case, it was found that when using a threshold score allowing prediction of 90% of the binders (i.e., imposing a required sensitivity of 0.9) was linked to an average efficiency (for all sizes) of 65.19%. That is, using a threshold that predicts 90% of the binders, 65.19% of the predictions are actually correct. Similarly, a threshold predicting 75% of all binders in the data set, generates predictions that are 79.28% efficient on average (79.28% of the predicted peptides are actual binders).

Identification of SIVmac239-derived Mamu-A*11-restricted epitopes

To identify SIV derived epitopes, SIVmac239 proteins were examined for sequences which matched the Mamu-A*11 primary anchor motif. Peptides with the negatively charged

Table 2 The relative influence of secondary anchor residues on Mamu-A*11 binding capacity

Residue	Position (ARB)										
	1	2	3	4	5	6	7	8	9	10	11
a. 8-mer peptides[a]											
A	**4.8**	*0.00001*	1.6	0.97	3.2	1.0	1.6	0.0069			
C	0.74	*0.00001*	0.69	0.65	0.26	0.64	0.47	*0.00001*			
D	*0.21*	0.021	0.31	0.35	*0.21*	0.49	0.51	*0.00001*			
E	*0.18*	***1.0***	0.39	1.1	0.43	1.4	0.86	*0.00001*			
F	**11**	*0.00001*	**4.5**	0.45	0.30	**4.0**	0.82	0.039			
G	**9.8**	*0.00001*	1.1	*0.20*	**11**	0.63	0.57	*0.00001*			
H	0.81	*0.00001*	1.8	1.7	3.3	0.34	0.72	*0.00001*			
I	0.68	*0.00001*	1.7	2.1	**4.1**	0.31	0.57	***1.0***			
K	0.53	*0.00001*	0.49	**5.5**	0.32	0.32	1.2	*0.00001*			
L	2.8	*0.00001*	2.9	**4.7**	1.6	0.87	**5.1**	0.057			
M	0.83	0.018	1.5	1.4	3.1	1.1	2.4	0.043			
N	*0.12*	*0.00001*	0.40	3.7	2.6	**12**	0.85	*0.00001*			
P	*0.12*	*0.00001*	0.48	0.34	0.83	0.37	0.89	*0.00001*			
Q	0.74	*0.00001*	*0.23*	1.4	0.54	0.37	0.85	*0.00001*			
R	1.2	*0.00001*	3.2	0.34	0.92	1.8	0.38	*0.00001*			
S	3.4	*0.00001*	1.7	0.62	0.28	0.30	*0.19*	*0.00001*			
T	0.33	*0.00001*	0.58	1.0	*0.25*	1.3	0.65	0.0063			
V	0.31	*0.00001*	0.66	*0.24*	3.8	2.5	1.9	0.072			
W	1.6	*0.00001*	**4.4**	0.90	*0.11*	1.3	0.85	0.018			
Y	**9.0**	*0.00001*	**5.5**	**17**	0.99	0.68	0.32	0.0032			
b. 9-mer peptides[b]											
A	**4.2**	*0.00001*	1.3	1.1	0.64	1.8	1.0	1.2	0.0069		
C	**4.3**	*0.00001*	0.77	0.88	0.51	*0.10*	**13**	0.30	*0.00001*		
D	*0.090*	0.021	0.26	0.88	*0.21*	*0.19*	0.45	1.0	*0.00001*		
E	*0.17*	***1.0***	0.57	1.4	0.62	0.94	2.0	0.67	*0.00001*		
F	0.86	*0.00001*	**6.4**	1.1	3.6	3.4	2.2	*0.23*	0.039		
G	2.9	*0.00001*	0.28	0.28	1.5	*0.25*	0.37	1.1	*0.00001*		
H	**4.0**	*0.00001*	2.4	*0.22*	2.5	0.47	2.9	1.9	*0.00001*		
I	1.4	*0.00001*	3.9	2.0	**6.9**	**6.2**	1.5	0.88	***1.0***		
K	2.7	*0.00001*	1.8	*0.25*	0.37	*0.21*	0.31	**11**	*0.00001*		
L	0.93	*0.00001*	1.5	3.8	1.0	1.4	1.2	3.4	0.057		
M	0.81	0.018	**37**	2.1	2.1	2.6	**14**	1.2	0.043		
N	0.35	*0.00001*	0.59	0.51	0.56	0.37	0.61	*0.054*	*0.00001*		
P	*0.082*	*0.00001*	*0.12*	*0.090*	1.9	1.8	1.4	0.62	*0.00001*		
Q	0.87	*0.00001*	0.27	2.6	0.53	1.1	0.49	2.9	*0.00001*		
R	2.5	*0.00001*	1.4	0.38	1.5	1.2	0.29	1.8	*0.00001*		
S	3.8	*0.00001*	1.1	**5.4**	2.1	1.5	0.56	2.6	*0.00001*		
T	*0.11*	*0.00001*	1.1	2.4	0.33	1.8	1.5	0.30	0.0063		
V	0.87	*0.00001*	1.9	2.0	1.1	**4.6**	0.96	0.67	0.072		
W	**15**	*0.00001*	**4.3**	1.3	3.2	1.2	1.5	0.56	0.018		
Y	3.1	*0.00001*	**4.8**	1.5	1.2	0.62	1.6	0.37	0.0032		
c. 10-mer peptides[c]											
A	**11**	*0.00001*	0.34	1.1	0.39	2.2	0.63	0.39	**4.2**	0.0069	
C	1.8	*0.00001*	0.52	1.4	*0.048*	1.1	**32**	1.1	2.1	*0.00001*	
D	*0.063*	0.021	1.7	*0.15*	0.95	*0.13*	0.88	1.1	0.40	*0.00001*	
E	*0.14*	***1.0***	0.47	2.4	0.40	1.1	0.76	0.60	0.58	*0.00001*	
F	**4.5**	*0.00001*	**5.8**	0.33	**5.1**	**23**	0.57	1.6	**8.0**	0.039	
G	0.99	*0.00001*	0.60	1.2	0.38	1.9	1.7	0.36	0.76	*0.00001*	
H	3.5	*0.00001*	0.43	1.6	**14**	0.35	0.45	*0.21*	2.7	*0.00001*	
I	0.49	*0.00001*	1.8	0.67	2.3	1.4	**5.2**	0.83	1.2	***1.0***	
K	3.5	*0.00001*	*0.21*	0.63	0.33	0.47	0.82	1.2	**4.0**	*0.00001*	
L	0.47	*0.00001*	**4.7**	0.57	1.2	1.3	0.88	0.71	0.68	0.057	

Table 2 (continued)

Residue	Position (ARB)										
	1	2	3	4	5	6	7	8	9	10	11
M	3.1	0.018	**7.3**	**7.2**	**15**	1.2	1.2	3.7	0.50	0.043	
N	0.69	*0.00001*	0.95	0.88	2.1	1.1	2.8	0.28	0.39	*0.00001*	
P	*0.11*	*0.00001*	*0.094*	2.1	0.74	1.1	2.1	2.2	0.29	*0.00001*	
Q	0.76	*0.00001*	2.7	0.28	0.53	0.35	2.6	3.2	*0.073*	*0.00001*	
R	**5.2**	*0.00001*	1.3	**11**	1.0	0.28	0.36	1.2	1.9	*0.00001*	
S	**18**	*0.00001*	1.7	1.4	2.1	1.2	*0.14*	1.7	3.9	*0.00001*	
T	0.74	*0.00001*	*0.086*	1.4	3.4	1.7	0.90	0.71	0.76	0.0063	
V	0.60	*0.00001*	0.37	0.51	1.3	1.1	1.5	0.34	0.71	0.072	
W	**6.1**	*0.00001*	**6.8**	0.79	1.2	*0.21*	0.35	**17**	0.39	0.018	
Y	1.4	*0.00001*	**11**	0.66	1.2	**13**	0.93	**12**	0.59	0.0032	
d. 11-mer peptides[d]											
A	3.0	*0.00001*	2.8	1.3	0.36	0.77	0.86	0.46	0.45	1.1	0.0069
C	0.44	*0.00001*	0.57	1.1	0.41	**4.1**	0.68	0.93	1.5	2.2	*0.00001*
D	*0.078*	0.021	0.43	3.1	0.91	*0.11*	0.35	*0.093*	*0.18*	0.48	*0.00001*
E	0.55	***1.0***	1.2	2.3	1.6	0.58	0.95	0.91	0.81	**4.7**	*0.00001*
F	1.7	*0.00001*	2.5	2.9	1.4	2.1	2.2	0.73	**4.0**	0.89	0.039
G	**6.6**	*0.00001*	0.49	1.6	0.40	0.78	*0.20*	0.92	0.29	1.0	*0.00001*
H	1.2	*0.00001*	0.59	0.46	3.3	**8.9**	0.79	1.1	0.92	1.1	*0.00001*
I	0.64	*0.00001*	0.42	0.40	0.94	1.4	0.51	3.5	0.43	0.41	**1.0**
K	2.3	*0.00001*	0.58	0.46	1.3	0.47	0.87	0.73	0.94	1.1	*0.00001*
L	1.8	*0.00001*	3.2	3.4	**4.8**	1.0	**13**	1.5	2.7	1.6	0.057
M	1.0	0.018	1.5	1.9	1.8	1.0	3.2	1.6	1.5	0.55	0.043
N	0.54	*0.00001*	0.92	0.29	3.6	*0.24*	1.5	**6.9**	1.9	0.44	*0.00001*
P	*0.14*	*0.00001*	0.74	0.30	0.65	*0.22*	0.63	0.78	0.47	0.43	*0.00001*
Q	0.80	*0.00001*	1.2	*0.23*	0.67	0.35	0.61	0.66	2.4	1.7	*0.00001*
R	2.4	*0.00001*	0.68	0.74	0.84	**8.6**	0.50	**7.1**	1.6	1.9	*0.00001*
S	0.75	*0.00001*	1.0	0.34	0.58	1.6	0.30	0.78	1.8	0.73	*0.00001*
T	0.44	*0.00001*	0.43	0.28	0.39	**14**	0.44	0.85	3.4	**5.5**	0.0063
V	0.79	*0.00001*	1.3	3.2	0.87	1.0	1.3	0.77	**6.0**	0.35	0.072
W	0.31	*0.00001*	1.4	**7.8**	1.4	2.2	1.9	0.72	2.3	0.59	0.018
Y	1.7	*0.00001*	1.5	0.50	1.4	0.48	2.9	2.8	1.5	3.6	*0.0032*

ARB values shown were calculated as described in the Materials and methods. ARB were derived for each residue considered individually when there were five or more occurences of that residue in the specified position in the database. When there were fewer than five occurences ARB calculations include data obtained for chemically similar amino acids. At secondary anchor positions values representing a fourfold or greater increase (corresponding to approximately one standard deviation) in binding capacity are indicated by *bold font*. Values corresponding to a fourfold or greater decrease in binding capacity are indicated by *italic font*. Main anchor positions are *shaded*, and residues determined to be preferred anchors are indicated by *bold italic font*. ARB values at the main anchor positions are derived from the analyses described in Table 1, and are indexed relative to the residue with the best binding capacity. To allow use of the values shown in this table as coefficients for predictive algorithms, the values for non-tolerated anchor residues have been set to 0.0001 to filter out non-motif peptides

[a]A panel of 214 8-mer peptides based on naturally occurring sequences from various viral, bacterial, or pathogen origin was analyzed. The average geometric binding capacity of the panel was 3,251 nM

[b]A panel of 370 9-mer peptides based on naturally occurring sequences from various viral, bacterial, or pathogen origin was analyzed. The average geometric binding capacity of the panel was 817 nM

[c]A panel of 277 10-mer peptides based on naturally occurring sequences from various viral, bacterial, or pathogen origin was analyzed. The average geometric binding capacity of the panel was 993 nM

[d]A panel of 192 11-mer peptides based on naturally occurring sequences from various viral, bacterial, or pathogen origin was analyzed. The average geometric binding capacity of the panel was 2,375 nM

residues E or D, or M, at the second position and I, V, L, M, F or W at the C-terminal positions were selected. Peptides with T, A, and Y at the C-terminus were also considered because noted in the library analysis, peptides with these residues can occasionally bind. In total, 656 peptides were selected for study.

Each of the 656 peptides were evaluated for their ability to bind to Mamu-A*11 in vitro using purified MHC molecules, as described in the Materials and methods. In total, 178 (27.1%) of the SIVmac239 peptides bound Mamu-A*11 with an $IC_{50} \leq 500$ nM. Of these, 85 peptides had binding affinities of 50 nM, or less. Of note, the previously

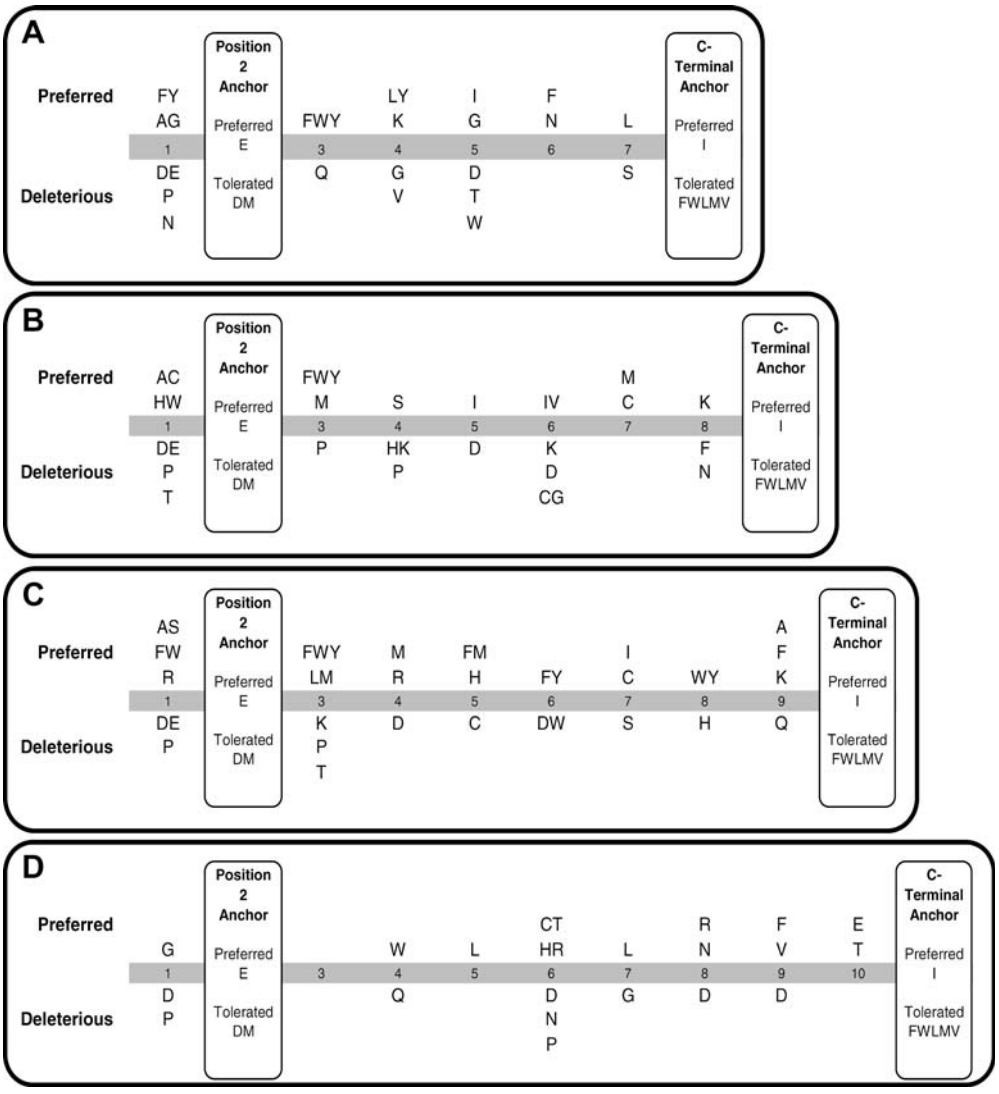

Fig. 2 Map of the Mamu-A*11 motif. Summary map of preferred and deleterious influences on Mamu A*11 binding capacity for 8- (**a**), 9- (**b**), 10- (**c**) and 11-mer (**d**) peptides. At secondary anchor positions, residues shown as preferred (or deleterious) are associated with ARB values at least fourfold greater than (or fourfold less than) peptides of the same size carrying other residues at the same position. At the primary anchor positions, preferred residues are those associated with an average binding capacity within tenfold of the optimal residue at the same position. See legend for Table 2 for additional details

well characterized Mamu-A*11-restricted CD8$^+$ T-cell epitope Env$_{495\text{-}502}$GI8 (Evans et al. 1999, 2000) bound to Mamu-A*11 with the second highest binding affinity (2.3 nM).

Table 3 Performance of a polynomial algorithm for predicting Mamu A*11 binders

Peptide size	Fraction of possible binders			
90%		75%		
Score[a]	Efficiency[b]	Score	Efficiency	
8	0.81	69.09	0.93	78.05
9	0.56	69.39	0.76	89.76
10	0.59	71.13	0.81	86.60
11	0.67	51.14	0.84	62.71
Average		65.19		79.28

[a]Indicates the algorithm score that allows selection of a set of peptides that includes 90% (or 75%) of the peptides in the data set that bound Mamu A*11 with an IC50 value of 500 nM or better

[b]Indicates the percentage of peptides in the set identified by the algorithm score that bind Mamu A*11 with an IC50 value of 500 nM or better

Antigenicity assays were next performed to identify epitopes targeted by Mamu-A*11-restricted CD8$^+$ T-cell responses. In particular, we evaluated whether SIV-derived Mamu-A*11 binders were recognized ex vivo by fresh PBMC from SIV-infected Mamu-A*11-positive animals in ELISPOT assays. Fresh PBMC from four Mamu-A*11-positive animals were reactive to 16 different peptides, seven of which were recognized in two or more animals (Fig. 3). Specifically, responses against these seven peptides resulted in net SFCs ranging from 50 to 660 per 1×10^6 cells. Not all the peptides were recognized by all of the animals, and considerable variability existed from animal to animal. To verify assay reproducibility, peptides associated with responses in the 50–100 SFCs range were retested using PBMC from the same animal.

All the animals recognized more than one peptide, including animal 95096, which recognized ten of the peptides, the largest repertoire of responses. The strongest response was detected with PBMC from animal 97089, with 660 SFCs per 1×10^6 cells to the Pol$_{507\text{-}517}$AI11 peptide. Pol$_{507\text{-}517}$AI11 was one of the shared responses (animals 95096 and 97089), as was the previously described

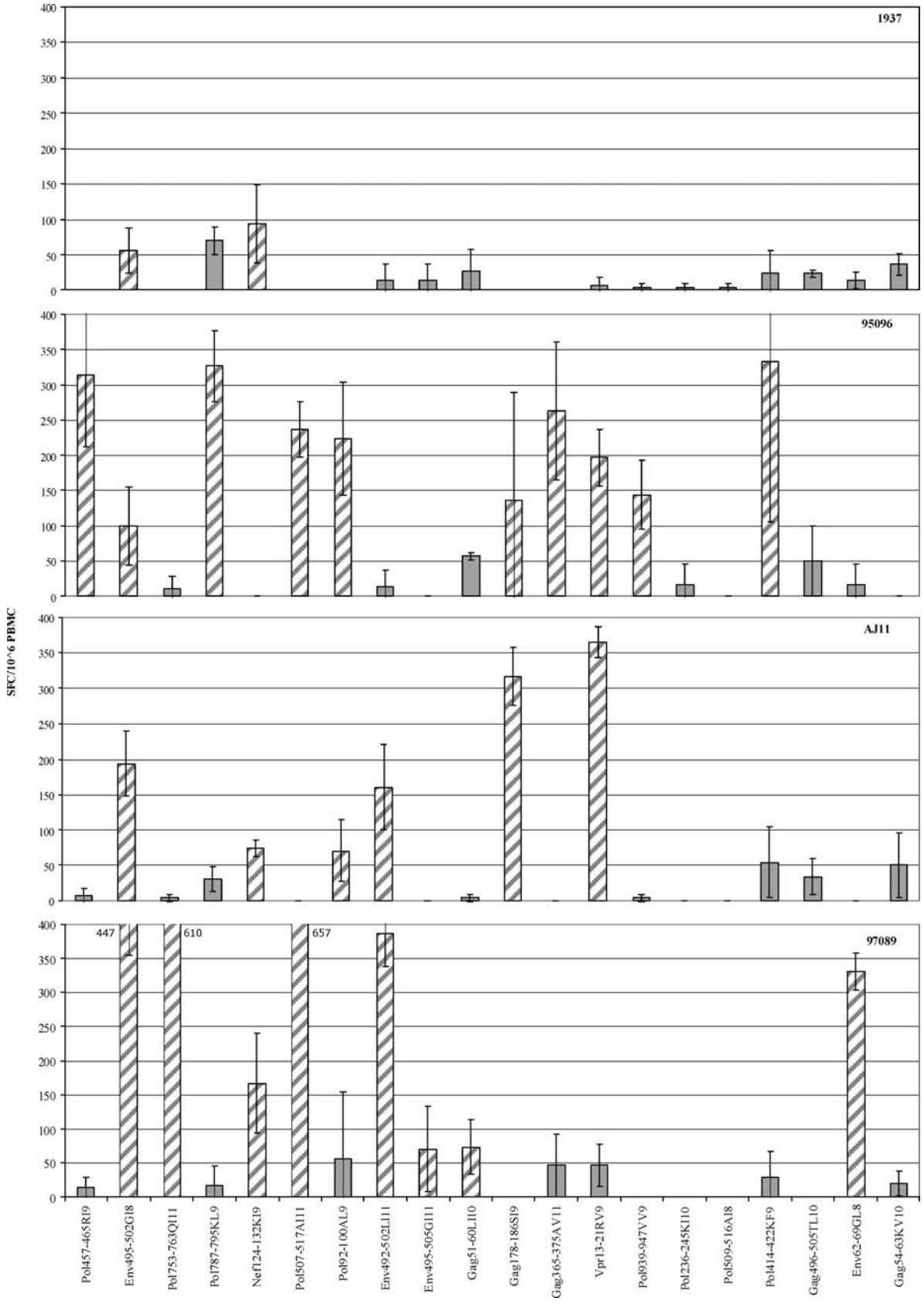

Fig. 3 Detection of IFN-γ production by rhesus macaque PBMC using the ELISPOT assay. PBMC from various Mamu-A*11 SIV-infected animals were tested with the Mamu-A*11 peptides in 16- to 20-h ELISPOT assays. PBMC were plated in 96-well plates at 1×10^5 cells/well and stimulated with various peptides (10 mM concentration). Mean values and standard deviations from triplicate wells were calculated for each assay, and SFCs were enumerated, as described in Materials and methods. Mean SFC values and standard deviations are shown for each peptide tested. Background (sample with no peptide) levels were subtracted from each peptide average. A response was considered positive if the average number of SFCs exceeded a threshold of 50 and the average of sample with no peptide plus 2 standard deviations. *Diagonal bars* indicate positive responses (see Materials and methods)

$Env_{495\text{-}502}$GI8 (Evans et al. 1999, 2000) (shared by all four animals, 1937, 95096, AJ11, and 97089), $Nef_{124\text{-}132}$KI9 (animals 1937, AJ11, and 97089), $Pol_{92\text{-}100}$AL9 (animals 95096 and AJ11), $Env_{492\text{-}502}$LI11 (animals AJ11 and 97089), $Gag_{178\text{-}186}$SI9 (animals 95096 and AJ11) and $Vpr_{13\text{-}21}$RV9 (animals 95096 and AJ11).

Of these seven $CD8^+$ T-cell responses, two were from Env, two from Pol, and one each from Gag, Vpr and Nef. Six of these are newly identified as $Env_{495\text{-}502}$GI8 was previously described (Evans et al. 2000). The $Env_{495\text{-}502}$GI8 sequence is contained within another epitope, $Env_{492\text{-}502}$ LI11, and therefore $Env_{492\text{-}502}$LI11 is not considered a unique epitope. Utilizing positivity in two animals as a stringent criteria for epitope confirmation, our studies identify a total of five new epitopes, as $Env_{495\text{-}502}$GI8 was previously described (Evans et al. 1999, 2000).

Of all the animals used in this study, only animal 95096 was previously immunized with a liposome construct, which failed to engender any immune responses after vaccination (Mothe et al. 2002a). All of the other animals were initially control animals for vaccine and pathogenesis studies. None of these animals were vaccinated prior and therefore, any control of viral replication would be due to natural immunity. Animals 95096 and 1937 were infected with SIV_{mac}239/nef open, receiving ten 50% monkey infectious doses, comprising approximately 3,000 50% tissue culture infective doses ($TCID_{50}$), intrarectally, as previously described (Allen et al. 2002a; Mothe et al. 2003; O'Connor et al. 2003). Animal 97089 was infected intravenously with 100 $TCID_{50}$ of the 3×SIV stock which is an engineered CTL variant virus based on SIV_{mac}239 (Friedrich et al. 2004). Animal AJ11 was infected three times with 300 $TCID_{50}$ SIV_{mac}239, intrarectally, before infection was detected (McDermott et al. 2004).

Mamu-A*01- and -B*17-positive animals generate SIV-specific responses, which we have previously shown to be correlated with viral control (Mothe et al. 2003; O'Connor et al. 2003). All four animals utilized in this study were Mamu-B*17-positive and three of them co-express Mamu-A*01, thus any correlates of immunity cannot be independently attributed to Mamu-A*11. However, it can be noted that animal AJ11 had low viral loads (less than 1,000 copies vRNA per ml of plasma) and two of the Mamu-A*11 animals were long-term non-progressors (animals 95096 and 1937) controlling viremia to undetectable levels. It is thus possible that Mamu-A*11-restricted immune responses in these animals contributed to this ability to restrain replication.

Mamu-A*11 peptide-binding specificity overlaps with those of H-2 K^k and the HLA B44-supertype

The Mamu-A*11 peptide-binding specificity is similar to the motif recognized by other MHC molecules, such as those of the HLA B44-supertype (Sette and Sidney 1999). We have previously reported that naturally processed HLA B*4402 epitopes bind Mamu-A*11 with appreciable frequency (Dzuris et al. 2000). Interestingly, the peptide-binding motif for the mouse class I molecule H-2 K^k, characterized by a requirement for E in position 2 and I or V at the C-terminus (Burrows et al. 1996; Cossins et al. 1993; Stryhn et al. 1996), is also similar. In the next series of experiments, we examined whether an overlap in the repertoires Mamu-A*11 and H-2 K^k exists at the level of peptide binding.

For this purpose, we tested a panel of 186 peptides for binding to both Mamu-A*11 and H-2 K^k binding (Table 4). The peptides in the set tested were derived from natural sequences, and had E or D in position 2, and A, F, I. L, M, V, W, or Y at the C-terminus. As shown in Table 4a, 82 (44.1%) of the peptides bound (IC_{50}<500 nM) K^k, and 69 (37.1%) bound Mamu-A*11. A concordance of 70.4% was noted, as 48 (25.8%) peptides bound both molecules and 83 (44.6%) bound neither. Cross-reactivity between K^k and Mamu-A*11 was found to be fairly high, as 48 (46.6%) of the 103 peptides that bound at least one molecule bound both. H-2 K^k shared with Mamu-A*11 a preference for 9- and 10-mer

Table 4 Mamu-A*11 and H-2 K^k share overlapping peptide binding repertoires

H-2 K^k	Mamu A*11 binder		Total	
Binder	Yes	No		
a. Overall cross-reactivity (% binders)				
Yes	25.8	18.3	44.1	
No	11.3	44.6	55.9	
Total	37.1	62.9	100.0	
Concordance: 70.4				
Size	*n*	% Peptides binding		
		Mamu A*11	H-2 K^k	Both
b. Peptide length				
8	51	23.5	39.2	17.6
9	101	39.6	44.6	28.7
10	26	61.5	57.7	38.5
11	8	12.5	25.0	0.0
Total	186	37.1	44.1	25.8
Residue	*n*	% Peptides binding		
		Mamu A*11	H-2 K^k	Both
c. Position 2				
D	50	6.0	12.0	2.0
E	136	48.5	55.9	34.6
Total	186	37.1	44.1	25.8
Residue	*n*	% Peptides binding		
		Mamu A*11	H-2 K^k	Both
d. C-terminus				
A	22	13.6	13.6	4.5
F	18	44.4	44.4	27.8
I	34	61.8	73.5	61.8
L	51	39.2	43.1	17.6
M	6	16.7	33.3	0.0
V	30	43.3	60.0	36.7
W	9	0.0	11.1	0.0
Y	15	20.0	13.3	6.7
Total	186	37.1	44.1	25.8

Table 5 SIV Mamu A*11 epitopes can be recognized in the context of H-2 K^k

Peptide	Sequence	Mamu-A*11 binding capacity (IC50 nM)	Response to peptide by Mamu-A*11 ELISPOT	K^k Binding capacity (IC50 nM)	Response to peptide by K^k ELISPOT
Gag 178-186SI9	SEGCTPYDI	34	+	17	+
Pol 507-517AI11	AEAEYEENKII	5.2	+	69	+
Env 492-502LI11	LELGDYKLVEI	5.4	+	459	+
Env 495-502GI8	GDYKLVEI	0.62	+	5274	−
Vpr 13-21RV9	REPWDEWVV	50	+	>50000	−
Pol 939-947VV9	VETIVLMAV	56	−	67	−
Pol 753-763QI11	QEIDHLVSQGI	3.9	−	114	−
Gag 365-375AV11	AEALKEALAPV	48	−	4578	−
Pol 414-422KF9	KELLNSIGF	110	−	24019	−
Gag 54-63KV10	KEGCQKILSV	295	−	24580	−
Gag 51-60LI10	LENKEGCQKI	12	−	71	+

peptides, although 8- and 11-mers were also tolerated (Table 4b).

Analysis of the patterns of binding with respect to the residues in the primary anchor positions reveal a remarkable degree of similarity in the preferences of H-2 K^k and Mamu-A*11. Both molecules showed an overwhelming preference for E in position 2 (Table 4c) and I at the C-terminus (Table 4d). More specifically, 48.5% of the peptides with E in position 2 bound Mamu-A*11, and 55.9% bound K^k; 34.6% of the peptides bound both molecules. Preferences at the C-terminus were also shared between H-2 K^k and Mamu-A*11, where it was found that 73.5% of the peptides with I at the C-terminus bound K^k, and 61.8% bound Mamu-A*11. Consistent with the reported motif for K^k, peptides with V at the C-terminus were frequently (60%) K^k binders. As with Mamu-A*11, but not previously reported for K^k, K^k also well-tolerated the hydrophobic and/or aliphatic residues F, L, and M, at the C-terminus, with between 33 and 44% of the peptides with these residues binding. Peptides with the small residue A, or the large aromatic residues W and Y, bound H-2 K^k and Mamu-A*11, but with considerably less frequency. Taken together, these data demonstrate a significant overlap in the peptide binding specificities and repertoires of H-2 K^k and Mamu-A*11, and also reveal that H-2 K^k recognizes a somewhat broader main anchor motif than previously reported.

Immunogenicity of Mamu-A*11 binding epitopes in H-2K^k mice

To substantiate the biological relevance of this cross-reactivity, we tested a panel of 11 Mamu-A*11 binders for their immunogenicity in H-2 K^k mice. Groups of three mice were immunized with a mixture of peptides consisting of seven class I-restricted peptides and two class II-restricted peptides. Two different mixtures were prepared and delivered subcutaneously (see Materials and methods). After 11-14 days, mice were sacrificed and splenocytes purified for subsequent ELISPOT analysis. Six of the 11 peptides tested were K^k binders (Table 5). Of these, four peptides were immunogenic in the K^k mice (Fig. 4), and all them were also noted to have K^k binding affinities better than 500 nM. The magnitude of responses ranged from 125 to 695 SFCs p/1×10^6 cells. None of the four peptides that did not bind K^k were immunogenic. Of six Mamu-A*11 binders that also bound K^k, four were immunogenic in K^k mice. Our antigen presenting cells posses a full complement of K haplotype molecules. Thus, it is possible that another class I molecule may restrict the responses. This, however, appears unlikely, in light of the fact that the specificity of D^k appears to be diametrically opposed [amino acid R in position 2 (Lukacher and Wilson 1998; Wilson et al. 1999)].

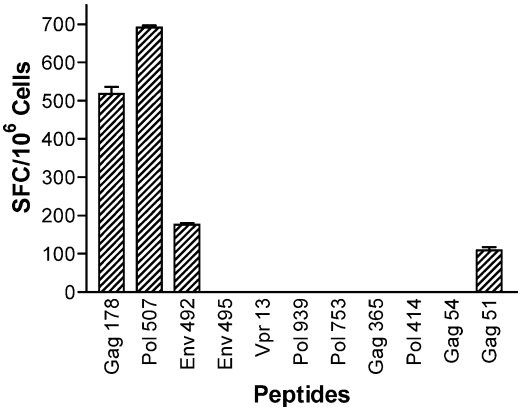

Fig. 4 $CD8^+$ (IFN-γ) responses specific for class I-restricted epitopes. CBA mice were immunized with a mixture of peptides as described in the Materials and methods. Eleven to 14 days after immunization, purified $CD8^+$ splenocytes from primed animals were utilized in ELISPOT assays. This is a representative example of two independent experiments. To determine the level of significance, a Student's *t*-test was performed in which $P \leq 0.05$ using the mean of triplicate values of immunized mice (relevant peptide response-irrelevant peptide response) versus unimmunized mice (relevant peptide response-irrelevant peptide response)

Of significant note was that three of four immunogenic peptides were also recognized in infected Mamu A*11 animals. These data suggest that testing the immunogenicity in K^k mice of Mamu-A*11/K^k cross-reactive binders maybe provide a small-laboratory animal model to predict immunogenicity for Mamu-A*11 positive macaques.

Discussion

Animal models are instrumental in pathogenesis studies and in evaluating novel vaccines. However, the immunogenetics and immunochemistry of only a limited number of animal species has been analyzed in detail. Consequently, the molecular tools necessary (such as tetrameric staining reagents) to measure cellular responses, and to evaluate correlates of protection after infection or vaccination, are available in few select animal models and immunogenetic backgrounds. In the context of the rhesus macaque, an important disease model for HIV and other infectious diseases, we have previously investigated the peptide binding specificity of two MHC class I molecules, Mamu-A*01 and Mamu-B*17, and two MHC class II molecules, Mamu DRBw*201 and Mamu DRB1*0406 (Allen et al. 2001; Dzuris et al. 2001; Mothe et al. 2002b; Sidney et al. 2000). These studies resulted in the identification of a number of SIV-derived CTL and HTL epitopes which have subsequently been utilized in vaccine studies, and in studies aiming to understand natural correlates of protection (Allen et al. 2000a, 2002a,b; Mothe et al. 2002a; O'Connor et al. 2002, 2003). In the present study, we have extended our systematic analysis of rhesus macaque alleles to include the class I molecule Mamu-A*11.

We found that Mamu-A*11 molecules preferentially bind peptides of 9 or 10 residues in length, although 8- and 11-mers ligands also bind with reasonable frequency. Similar to most other class I molecules studied to date, Mamu-A*11 utilizes the residues in position 2 and at the C-terminus of its peptide ligands as the main anchors determining binding capacity. At position 2 the acidic residue E was preferred, and D was tolerated. Surprisingly, the large aliphatic residue M (but not other aliphatic residues) was also tolerated. This appears to be a unique feature of the Mamu-A*11 molecule and was unexpected on the basis of the specificity of other MHC molecules that also bind peptides with negatively charged residues in position 2 (Rammensee et al. 1999; Sette and Sidney 1998, 1999; Sidney et al. 1996a, 2003). This result underscores the usefulness of comprehensive studies utilizing quantitative binding measures and purified MHC molecules for the definition of accurate MHC-peptide binding motifs. At the C-terminus, I is preferred, and the hydrophobic residues F, W, L, M and V are tolerated. This specificity resembles that at the C-terminus of many other MHC molecules, including those of the HLA-B7 and -B44-supertypes (Sidney et al. 1996c, 2003).

Residues in secondary anchor positions also influence the capacity of peptides to bind Mamu-A*11. Analysis of these influences have allowed the derivation of detailed motifs, and served as the basis of polynomial algorithms for predicting Mamu-A*11 binding capacity. A typical limitation of algorithms with the capacity to account for secondary interactions is that they are applicable only in the case of 9- and 10-mer sequences. However, as demonstrated above, peptides of 8 or 11 residues can also frequently bind class I molecules, and many 8- and 11-mer epitopes have been identified in a number of contexts (Rammensee et al. 1999). The present analysis has provided a predictive method that is applicable for sequences between 8 and 11 residues. We found that our polynomial algorithms can predict about 75% of the binders, with 75% accuracy. This level of performance is relatively good, compared with the performance of other algorithms (Doolan et al. 2003; Gulukota et al. 1997; Peters et al. 2003; Udaka et al. 2000, 2002).

We anticipate that predictive algorithms will be useful in the study of Category A-C pathogens. Reliable identification of the immunodominant epitopes will enable production of tetrameric reagents, the performance of rigorous immunopathology studies, and the testing of potential vaccine candidates.

Characterization of the peptide-binding specificity of Mamu-A*11 in conjunction with the use of high-throughput Mamu-A*11 peptide-binding assays has allowed us to identify over 175 peptides derived from SIV antigens that bind Mamu-A*11 with high affinity (IC_{50}<500 nM). Further analyses of these peptides using ELISPOT assays with PBMC from SIV-infected animals indicated that six of these peptides had the capacity to reproducibly elicit recall $CD8^+$ T-cell responses from multiple animals. One of the responses was directed against the previously defined $Env_{495\text{-}502}$GI8 epitope (Evans et al. 1999). Therefore, five novel SIV $CD8^+$ T-cell epitopes were identified in these studies. A broad repertoire of $CD8^+$ T-cell responses has been previously demonstrated in the course of SIV infection in the context of other rhesus macaque class I molecules (Allen et al. 2001; Mothe et al. 2002b), as well as in humans infected with HIV (McMichael and Phillips 1997; Rowland-Jones et al. 1998), influenza (Gianfrani et al. 2000; Jameson et al. 1998), HBV (Chisari and Ferrari 1995) and HCV (Chang et al. 1999; Cooper et al. 1999; Koziel et al. 1995; Rehermann et al. 1996; Scognamiglio et al. 1999). The present results solidify the concept that broad and diverse T-cell receptor responses are commonly observed in primates (human and non-human), and raise doubts about the general applicability of the strict immunodominance observed in the case inbred strains of mice.

To date, only two Indian rhesus macaque MHC class I molecules, Mamu-A*01 and Mamu-B*17, have been intensely investigated. As a result of the limited amount of information regarding the specificity of macaque MHC, a shortage of genetically defined animals now exists (Allen et al. 1998, 2000a,b, Allen et al. 2001; Chen et al. 1992, 2000; Egan et al. 1999; Furchner et al. 1999; Hanke et al. 1998; Hel et al. 2000, 2001; Knapp et al. 1997; Kuroda et al. 1998, 1999; Mothe et al. 2002a,b, 2003; O'Connor et al. 2003; Schmitz et al. 2000; Veazey et al. 2001). The detailed characterization of the specificity of other Mamu

class I molecules, in this case Mamu-A*11, is expected to alleviate the demand for genetically defined macaques.

The reported Mamu-A*11 peptide binding specificity overlaps with that of H-2 K^k (Burrows et al. 1996; Cossins et al. 1993; Stryhn et al. 1996) and the HLA-B44-supertype (Sette and Sidney 1999; Sidney et al. 2003). We have previously demonstrated that naturally processed HLA-B*44 epitopes can bind Mamu-A*11 molecules (Dzuris et al. 2000). In the present study we performed K^k binding assays and demonstrated that the peptide binding repertoire of K^k overlaps significantly that of with Mamu-A*11. Indeed, almost 50% of the peptides that bound either molecule bound both. Mamu-A*11 shares an identical F pocket structure with Kk, and an identical B pocket structure with the HLA B44-supertype molecules B*4001, B*4002, and B*4501. This observation is consistent with previous observation that suggested that MHC molecules with similar pocket structures will often share similar binding specificity in that pocket [see Sette and Sidney (1999) for review].

While this data is not entirely unexpected, the demonstration of this phenomenon suggests novel utility in the context of vaccine development. Interspecies cross-reactivity was also demonstrated at the T-cell repertoire level. Importantly, 3/4 Mamu-A*11 binders which were immunogenic in K^k in mice were also immunogenic in SIV-infected animals. Thus, given the overlap in repertoires noted between these two molecules, our results indicate that in certain contexts it may be possible to perform initial studies in mice before escalating to the more laborious and expensive macaques.

In summary, we have characterized, in depth, the peptide binding specificity of the rhesus macaque class I molecule Mamu-A*11, and generated an algorithm for identifying new Mamu-A*11-restricted epitopes. Our studies have also led to the identification of five novel SIV-derived $CD8^+$ T-cell epitopes restricted by Mamu-A*11. Finally, we have demonstrated that cross-reactivity may exist between Mamu-A*11 and the mouse class I molecule K^k.

Acknowledgements We thank Tim Jacoby and William Rehrauer, Ph.D., for the PCR-SSP typing and the Immunology and Virology Core Laboratories at the National Primate Research Center, University of Wisconsin-Madison for technical assistance. This work was supported by grant R24 RR15371 (D.I.W.) from the National Institutes of Health, NIH-NIAID contracts NO1-AI-95362 (A.S.) and HHSN266200400006C (A.S)

References

Allen TM, Jing P, Calore B, Horton H, O'Connor DH, Hanke T, Piekarczyk M, Ruddersdorf R, Mothe BR, Emerson C, Wilson N, Lifson JD, Belyakov IM, Berzofsky JA, Wang C, Allison DB, Montefiori DC, Desrosiers RC, Wolinsky S, Kunstman KJ, Altman JD, Sette A, McMichael AJ, Watkins DI (2002a) Effects of cytotoxic T lymphocytes (CTL) directed against a single simian immunodeficiency virus (SIV) Gag CTL epitope on the course of SIVmac239 infection. J Virol 76:10507–10511

Allen TM, Mortara L, Mothe BR, Liebl M, Jing P, Calore B, Piekarczyk M, Ruddersdorf R, O'Connor DH, Wang X, Wang C, Allison DB., Altman JD, Sette A, Desrosiers RC, Sutter G, Watkins DI (2002b) Tat-vaccinated macaques do not control simian immunodeficiency virus SIVmac239 replication. J Virol 76:4108–4112

Allen TM, Mothe BR, Sidney J, Jing P, Dzuris JL, Liebl ME, Vogel TU, O'Connor DH, Wang X, Wussow MC, Thomson JA, Altman JD, Watkins DI, Sette A (2001) CD8(+) lymphocytes from simian immunodeficiency virus-infected rhesus macaques recognize 14 different epitopes bound by the major histocompatibility complex class I molecule mamu-A*01: implications for vaccine design and testing. J Virol 75:738–749

Allen TM, O'Connor DH, Jing P, Dzuris JL, Mothe BR, Vogel TU, Dunphy E, Liebl ME, Emerson C, Wilson N, Kunstman KJ, Wang X, Allison DB, Hughes AL, Desrosiers RC, Altman JD, Wolinsky SM, Sette A, Watkins DI (2000a) Tat-specific cytotoxic T lymphocytes select for SIV escape variants during resolution of primary viraemia. Nature 407:386–390

Allen TM, Sidney J, del Guercio MF, Glickman RL, Lensmeyer GL, Wiebe DA, DeMars R, Pauza CD, Johnson RP, Sette A, Watkins DI (1998) Characterization of the peptide binding motif of a rhesus MHC class I molecule (Mamu-A*01) that binds an immunodominant CTL epitope from simian immunodeficiency virus. J Immunol 160:6062–6071

Allen TM, Vogel TU, Fuller DH, Mothe BR, Steffen S, Boyson JE, Shipley T, Fuller J, Hanke T, Sette A, Altman JD, Moss B, McMichael AJ, Watkins DI (2000b) Induction of AIDS virus-specific CTL activity in fresh, unstimulated peripheral blood lymphocytes from rhesus macaques vaccinated with a DNA prime/modified vaccinia virus Ankara boost regimen. J Immunol 164:4968–4978

Barouch DH, Kunstman J, Glowczwskie J, Kunstman KJ, Egan MA, Peyerl FW, Santra S, Kuroda MJ, Schmitz JE, Beaudry K, Krivulka GR, Lifton MA, Gorgone DA, Wolinsky SM, Letvin NL (2003) Viral escape from dominant simian immunodeficiency virus epitope-specific cytotoxic T lymphocytes in DNA-vaccinated rhesus monkeys. J Virol 77:7367–7375

Barouch DH, Santra S, Schmitz JE, Kuroda MJ, Fu TM, Wagner W, Bilska M, Craiu A, Zheng XX, Krivulka GR, Beaudry K, Lifton MA, Nickerson CE, Trigona WL, Punt K, Freed DC, Guan L, Dubey S, Casimiro D, Simon A, Davies ME, Chastain M, Strom TB, Gelman RS, Montefiori DC, Lewis MG (2000) Control of viremia and prevention of clinical AIDS in rhesus monkeys by cytokine-augmented DNA vaccination. Science 290:486–492

Brander C, Walker BD (1999) Tlymphocyte responses in HIV-1 infection: implications for vaccine development. Curr Opin Immunol 11:451–459

Burrows GG, Ariail K, Celnik B, Gambee JE, Bebo BF Jr, Offner H, Vandenbark AA (1996) Variation in H-2K(k) peptide motif revealed by sequencing naturally processed peptides from T-cell hybridoma class I molecules. J Neurosci Res 45:803–811

Chang KM, Gruener NH, Southwood S, Sidney J, Pape GR, Chisari FV, Sette A (1999) Identification of HLA-A3 and -B7-restricted CTL response to hepatitis C virus in patients with acute and chronic hepatitis C. J Immunol 162:1156–1164

Chen ZW, Craiu A, Shen L, Kuroda MJ, Iroku UC, Watkins DI, Voss G, Letvin NL (2000) Simian immunodeficiency virus evades a dominant epitope-specific cytotoxic T lymphocyte response through a mutation resulting in the accelerated dissociation of viral peptide and MHC class I. J Immunol 164:6474–6479

Chen ZW, Shen L, Miller MD, Ghim SH, Hughes AL, Letvin NL (1992) Cytotoxic T lymphocytes do not appear to select for mutations in an immunodominant epitope of simian immunodeficiency virus gag. J Immunol 149:4060–4066

Chisari FV, Ferrari C (1995) Hepatitis B virus immunopathogenesis. Annu Rev Immunol 13:29–60

Cooper S, Erickson AL, Adams EJ, Kansopon J, Weiner AJ, Chien DY, Houghton M, Parham P, Walker CM (1999) Analysis of a successful immune response against hepatitis C virus. Immunity 10:439–449

Cossins J, Gould K, Brownlee GG (1993) Peptides shorter than a minimal CTL epitope may have a higher binding affinity than the epitope for the class I Kk molecule. Virology 195:851–854

Doolan DL, Southwood S, Freilich DA, Sidney J, Graber NL, Shatney L, Bebris L, Florens L, Dobano C, Witney AA, Appella E, Hoffman SL, Yates JR III, Carucci DJ, Sette A (2003) Identification of Plasmodium falciparum antigens by antigenic analysis of genomic and proteomic data. Proc Natl Acad Sci USA 100: 9952–9957

Dzuris JL, Sidney J, Appella E, Chesnut RW, Watkins DI, Sette A (2000) Conserved MHC class I peptide binding motif between humans and rhesus macaques. J Immunol 164:283–2891

Dzuris JL, Sidney J, Horton H, Correa R, Carter D, Chesnut RW, Watkins DI, Sette A (2001) Molecular determinants of peptide binding to two common rhesus macaque major histocompatibility complex class II molecules. J Virol 75:10958–10968

Egan MA, Kuroda MJ, Voss G, Schmitz JE, Charini WA, Lord CI, Forman MA, Letvin NL (1999) Use of major histocompatibility complex class I/peptide/beta2M tetramers to quantitate CD8(+) cytotoxic T lymphocytes specific for dominant and nondominant viral epitopes in simian-human immunodeficiency virus-infected rhesus monkeys. J Virol 73:5466–5472

Evans DT, Jing P, Allen TM, O'Connor DH, Horton H, Venham JE, Piekarczyk M, Dzuris J, Dykhuzen M, Mitchen J, Rudersdorf RA, Pauza CD, Sette A, Bontrop RE, DeMars R, Watkins DI (2000) Definition of five new simian immunodeficiency virus cytotoxic T-lymphocyte epitopes and their restricting major histocompatibility complex class I molecules: evidence for an influence on disease progression [In Process Citation]. J Virol 74:7400–7410

Evans DT, O'Connor DH, Jing P, Dzuris JL, Sidney J, da Silva J, Allen TM, Horton H, Venham JE, Rudersdorf RA, Vogel T, Pauza CD, Bontrop RE, DeMars R, Sette A, Hughes AL, Watkins DI (1999) Virus-specific cytotoxic T-lymphocyte responses select for amino-acid variation in simian immunodeficiency virus Env and Nef. Nat Med 5:1270–1276

Falk K, Rotzschke O, Stevanovic S, Jung G, Rammensee HG (1991) Allele-specific motifs revealed by sequencing of self-peptides eluted from MHC molecules. Nature 351:290–296

Friedrich TC, Dodds EJ, Yant LJ, Vojnov L, Rudersdorf R, Cullen C, Evans DT, Desrosiers RC, Mothe BR, Sidney J, Sette A, Kunstman K, Wolinsky S, Piatak M, Lifson J, Hughes AL, Wilson N, O'Connor DH, Watkins DI (2004) Reversion of CTL escape-variant immunodeficiency viruses in vivo. Nat Med 10: 275–281

Furchner M, Erickson AL, Allen T, Watkins DI, Sette A, Johnson PR, Walker CM (1999) The simian immunodeficiency virus envelope glycoprotein contains two epitopes presented by the Mamu-A*01 class I molecule. J Virol 73:8035–8039

Gianfrani C, Oseroff C, Sidney J, Chesnut RW, Sette A (2000) Human memory CTL response specific for influenza A virus is broad and multispecific. Hum Immunol 61:438–452

Goulder P, Price D, Nowak M, Rowland-Jones S, Phillips R, McMichael A (1997) Co-evolution of human immunodeficiency virus and cytotoxic T-lymphocyte responses. Immunol Rev 159:17–29

Gulukota K, Sidney J, Sette A, DeLisi C (1997) Two complementary methods for predicting peptides binding major histocompatibility complex molecules. J Mol Biol 267:1258–1267

Hanke T, Schneider J, Gilbert SC, Hill AVS, McMichael A (1998) DNA multi-CTL epitope vaccines for HIV and *Plasmodium falciparum*—immunogenicity in mice. Vaccine 16:426–435

Hel Z, Nacsa J, Kelsall B, Tsai WP, Letvin N, Parks RW, Tryniszewska E, Picker L, Lewis MG, Edghill-Smith Y, Moniuszko M, Pal R, Stevceva L, Altman JD, Allen TM, Watkins D, Torres JV, Berzofsky JA, Belyakov IM, Strober W, Franchini G (2001) Impairment of Gag-specific CD8(+) T-cell function in mucosal and systemic compartments of simian immunodeficiency virus mac251- and simian-human immunodeficiency virus KU2-infected macaques. J Virol 75:11483–1495

Hel Z, Venzon D, Poudyal M, Tsai WP, Giuliani L, Woodward R, Chougnet C, Shearer G, Altman JD, Watkins D, Bischofberger N, Abimiku A, Markham P, Tartaglia J, Franchini G (2000) Viremia control following antiretroviral treatment and therapeutic immunization during primary SIV251 infection of macaques. Nat Med 6:1140–1146

Jameson J, Cruz J, Ennis FA (1998) Human cytotoxic T-lymphocyte repertoire to influenza A viruses. J Virol 72:8682–8689

Kast WM, Brandt RM, Sidney J, Drijfhout JW, Kubo RT, Grey HM, Melief CJ, Sette A (1994) Role of HLA-A motifs in identification of potential CTL epitopes in human papillomavirus type 16 E6 and E7 proteins. J Immunol 152:3904–3912

Klinman DM (1994) ELISPOT assay to detect cytokine-secreting murine and human cells. Curr Protoc Immunol 6:1–8

Knapp LA, Lehmann E, Piekarczyk MS, Urvater JA, Watkins DI (1997) A high frequency of Mamu-A*01 in the rhesus macaque detected by polymerase chain reaction with sequence-specific primers and direct sequencing. Tissue Antigens 50:657–6561

Kondo A, Sidney J, Southwood S, del Guercio MF, Appella E, Sakamoto H, Celis E, Grey HM, Chesnut RW, Kubo RT et al (1995) prominent roles of secondary anchor residues in peptide binding to HLA-A24 human class I molecules. J Immunol 155: 4307–4312

Kondo A, Sidney J, Southwood S, del Guercio MF, Appella E, Sakamoto H, Grey HM, Celis E, Chesnut RW, Kubo RT, Sette A (1997) Two distinct HLA-A*0101-specific submotifs illustrate alternative peptide binding modes. Immunogenetics 45:249–258

Koziel MJ, Dudley D, Afdhal N, Grakoui A, Rice CM, Choo QL, Houghton M, Walker BD (1995) HLA class I-restricted cytotoxic T lymphocytes specific for hepatitis C virus. Identification of multiple epitopes and characterization of patterns of cytokine release. J Clin Invest 96:2311–2321

Kubo RT, Sette A, Grey HM, Appella E, Sakaguchi K, Zhu NZ, Arnott D, Sherman N, Shabanowitz J, Michel H et al (1994) Definition of specific peptide motifs for four major HLA-A alleles. J Immunol 152:3913–3924

Kuroda MJ, Schmitz JE, Barouch DH, Craiu A, Allen TM, Sette A, Watkins DI, Forman MA, Letvin NL (1998) Analysis of Gag-specific cytotoxic T lymphocytes in simian immunodeficiency virus-infected rhesus monkeys by cell staining with a tetrameric major histocompatibility complex class I-peptide complex. J Exp Med 187:1373–1381

Kuroda MJ, Schmitz JE, Charini WA, Nickerson CE, Lord CI, Forman MA, Letvin NL (1999) Comparative analysis of cytotoxic T lymphocytes in lymph nodes and peripheral blood of simian immunodeficiency virus-infected rhesus monkeys. J Virol 73:1573–1579

Letvin NL, Schmitz JE, Jordan HL, Seth A, Hirsch VM, Reimann KA, Kuroda MJ (1999) Cytotoxic T lymphocytes specific for the simian immunodeficiency virus. Immunol Rev 170:127–134

Lukacher AE, Wilson CS (1998) Resistance to polyoma virus-induced tumors correlates with CTL recognition of an immunodominant H-2Dk-restricted epitope in the middle T protein. J Immunol 160:1724–1734

McDermott AB, Mitchen J, Piaskowski S, De Souza I, Yant LJ, Stephany J, Furlott J, Watkins DI (2004) Repeated low-dose mucosal simian immunodeficiency virus SIVmac239 challenge results in the same viral and immunological kinetics as high-dose challenge: a model for the evaluation of vaccine efficacy in nonhuman primates. J Virol 78:3140–3144

McMichael AJ, Phillips RE (1997) Escape of human immunodeficiency virus from immune control. Annu Rev Immunol 15: 271–296

Mothe BR, Horton H, Carter DK, Allen TM, Liebl ME, Skinner P, Vogel TU, Fuenger S, Vielhuber K, Rehrauer W, Wilson N, Franchini G, Altman JD, Haase A, Picker LJ, Allison DB, Watkins DI (2002a) Dominance of CD8 responses specific for epitopes bound by a single major histocompatibility complex class I molecule during the acute phase of viral infection. J Virol 76:875–884

Mothe BR, Sidney J, Dzuris JL, Liebl ME, Fuenger S, Watkins DI, Sette A (2002b) Characterization of the peptide-binding specificity of Mamu-B*17 and identification of Mamu-B*17-restricted epitopes derived from simian immunodeficiency virus proteins. J Immunol 169:210–219

Mothe BR, Weinfurter J, Wang C, Rehrauer W, Wilson N, Allen TM, Allison DB, Watkins DI (2003) Expression of the major histocompatibility complex class I molecule Mamu-A*01 is associated with control of simian immunodeficiency virus SIVmac239 replication. J Virol 77:2736–2740

Muhl T, Krawczak M, Ten Haaft P, Hunsmann G, Sauermann U (2002) MHC class I alleles influence set-point viral load and survival time in simian immunodeficiency virus-infected rhesus monkeys. J Immunol 169:3438–3446

Murali-Krishna K, Altman JD, Suresh M, Sourdive DJ, Zajac AJ, Miller JD, Slansky J, Ahmed R (1998) Counting antigen-specific CD8 T cells: a reevaluation of bystander activation during viral infection. Immunity 8:177–187

O'Connor DH, Allen TM, Vogel TU, Jing P, DeSouza IP, Dodds E, Dunphy EJ, Melsaether C, Mothe B, Yamamoto H, Horton H, Wilson N, Hughes AL, Watkins DI (2002) Acute phase cytotoxic T lymphocyte escape is a hallmark of simian immunodeficiency virus infection. Nat Med 8:493–499

O'Connor DH, Mothe BR, Weinfurter JT, Fuenger S, Rehrauer WM, Jing P, Rudersdorf RR, Liebl ME, Krebs K, Vasquez J, Dodds E, Loffredo J, Martin S, McDermott AB, Allen TM, Wang C, Doxiadis GG, Montefiori DC, Hughes A, Burton DR, Allison DB, Wolinsky SM, Bontrop R, Picker LJ, Watkins DI (2003) Major histocompatibility complex class I alleles associated with slow simian immunodeficiency virus disease progression bind epitopes recognized by dominant acute-phase cytotoxic-T-lymphocyte responses. J Virol 77:9029–9040

Peters B, Tong W, Sidney J, Sette A, Weng Z (2003) Examining the independent binding assumption for binding of peptide epitopes to MHC-I molecules. Bioinformatics 19:1765–1772

Rammensee H, Bachmann J, Emmerich NP, Bachor OA, Stevanovic S (1999) SYFPEITHI: database for MHC ligands and peptide motifs. Immunogenetics 50:213–219

Rammensee HG, Friede T, Stevanoviic S (1995) MHC ligands and peptide motifs: first listing. Immunogenetics 41:178–228

Rehermann B, Chang KM, McHutchinson J, Kokka R, Houghton M, Rice CM, Chisari FV (1996) Differential cytotoxic T-lymphocyte responsiveness to the hepatitis B and C viruses in chronically infected patients. J Virol 70:7092–7102

Rowland-Jones SL, Dong T, Fowke KR, Kimani J, Krausa P, Newell H, Blanchard T, Ariyoshi K, Oyugi J, Ngugi E, Bwayo J, MacDonald KS, McMichael AJ, Plummer FA (1998) Cytotoxic T cell responses to multiple conserved HIV epitopes in HIV-resistant prostitutes in Nairobi [see comments]. J Clin Invest 102:1758–1765

Ruppert J, Sidney J, Celis E, Kubo RT, Grey HM, Sette A (1993) Prominent role of secondary anchor residues in peptide binding to HLA-A2.1 molecules. Cell 74:929–937

Schmitz JE, Kuroda MJ, Veazey RS, Seth A, Taylor WM, Nickerson CE, Lifton MA, Dailey PJ, Forman MA, Racz P, Tenner-Racz K, Letvin NL (2000) Simian immunodeficiency virus (SIV)-specific CTL are present in large numbers in livers of SIV-infected rhesus monkeys. J Immunol 164:6015–6019

Scognamiglio P, Accapezzato D, Casciaro MA, Cacciani A, Artini M, Bruno G, Chircu ML, Sidney J, Southwood S, Abrignani S, Sette A, Barnaba V (1999) Presence of effector $CD8^+$ T cells in hepatitis C virus-exposed healthy seronegative donors. J Immunol 162:6681–6689

Sette A, Sidney J (1998) HLA supertypes and supermotifs: a functional perspective on HLA polymorphism. Curr Opin Immunol 10:478–482

Sette A, Sidney J (1999) Nine major HLA class I supertypes account for the vast preponderance of HLA-A and -B polymorphism. Immunogenetics 50:201–212

Sidney J, del Guercio MF, Southwood S, Engelhard VH, Appella E, Rammensee HG, Falk K, Rotzschke O, Takiguchi M, Kubo RT et al (1995) Several HLA alleles share overlapping peptide specificities. J Immunol 154:247–259

Sidney J, Dzuris JL, Newman MJ, Johnson RP, Kaur A, Amitinder K, Walker CM, Appella E, Mothe B, Watkins DI, Sette A (2000) Definition of the Mamu A*01 peptide binding specificity: application to the identification of wild-type and optimized ligands from simian immunodeficiency virus regulatory proteins. J Immunol 165:6387–6399

Sidney J, Grey HM, Kubo RT, Sette A (1996a) Practical, biochemical and evolutionary implications of the discovery of HLA class I supermotifs. Immunol Today 17:261–266

Sidney J, Grey HM, Southwood S, Celis E, Wentworth PA, del Guercio MF, Kubo RT, Chesnut RW, Sette A (1996b) Definition of an HLA-A3-like supermotif demonstrates the overlapping peptide-binding repertoires of common HLA molecules. Hum Immunol 45:79–93

Sidney J, Southwood S, del Guercio MF, Grey HM, Chesnut RW, Kubo RT, Sette A (1996c) Specificity and degeneracy in peptide binding to HLA-B7-like class I molecules. J Immunol 157:3480–3490

Sidney J, Southwood S, Oseroff C, del Guercio MF, Sette A, Grey HM (1998) Measurement of MHC/peptide interactions by gel filtration. Current Protocols in Immunolgy, Wiley, New York, 18.3.1–18.3.19

Sidney J, Southwood S, Mann DL, Fernandez-Vina MA, Newman MJ, and Sette A (2001) Majority of peptides binding HLA-A*0201 with high affinity crossreact with other A2-supertype molecules. Hum Immunol 62:1200–1216

Sidney J, Southwood S, Pasquetto V, Sette A (2003) Simultaneous prediction of binding capacity for multiple molecules of the HLA B44 supertype. J Immunol 171:5964–5974

Southwood S, Sidney J, Kondo A, del Guercio MF, Appella E, Hoffman S, Kubo RT, Chesnut RW, Grey HM, Sette A (1998) Several common HLA-DR types share largely overlapping peptide binding repertoires. J Immunol. 160:3363–3373

Stryhn A, Andersen PS, Pedersen LO, Svejgaard A, Holm A, Thorpe CJ, Fugger L, Buus S, Engberg J (1996) Shared fine specificity between T-cell receptors and an antibody recognizing a peptide/major histocompatibility class I complex. Proc Natl Acad Sci USA 93:10338–10342

Subbramanian RA, Kuroda MJ, Charini WA, Barouch DH, Costantino C, Santra S, Schmitz JE, Martin KL, Lifton MA, Gorgone DA, Shiver JW, Letvin NL (2003) Magnitude and diversity of cytotoxic-T-lymphocyte responses elicited by multiepitope DNA vaccination in rhesus monkeys. J Virol 77:10113–10118

Udaka K, Mamitsuka H, Nakaseko Y, Abe N (2002) Empirical evaluation of a dynamic experiment design method for prediction of MHC class I-binding peptides. J Immunol 169:5744–5753

Udaka K, Wiesmuller KH, Kienle S, Jung G, Tamamura H, Yamagishi H, Okumura K, Walden P, Suto T, Kawasaki T (2000) An automated prediction of MHC class I-binding peptides based on positional scanning with peptide libraries. Immunogenetics 51:816–828

Van Bleek GM, Nathenson SG (1990) Isolation of an endogenously processed immunodominant viral peptide from the class I H-2Kb molecule. Nature 348:213–216

Veazey RS, Gauduin MC, Mansfield KG, Tham IC, Altman JD, Lifson JD, Lackner AA, Johnson RP (2001) Emergence and kinetics of simian immunodeficiency virus-specific CD8(+) T cells in the intestines of macaques during primary infection. J Virol 75:10515–10519

Vogel TU, Friedrich TC, O'Connor DH, Rehrauer W, Dodds EJ, Hickman H, Hildebrand W, Sidney J, Sette A, Hughes A, Horton H, Vielhuber K, Rudersdorf R, De Souza IP, Reynolds MR, Allen TM, Wilson N, Watkins DI (2002) Escape. in one of two cytotoxic T-lymphocyte epitopes bound by a high-frequency major histocompatibility complex class I molecule, Mamu-A*02: a paradigm for virus evolution and persistence? J Virol 76:11623–11636

Wilson CS, Moser JM, Altman JD, Jensen PE, Lukacher AE (1999) Cross-recognition of two middle T protein epitopes by immunodominant polyoma virus-specific CTL. J Immunol 162:3933–3941